Supporting Information

Surface-layer Immobilization of Hydrophobic Pd-Porphyrin on Core–Shell Supports and Its Enhanced Photocatalytic Performance

Contents

1. Comparison before and after calcination

To quantify the chitosan (CTS) loading and verify the formation of a thermally stable, condensed shell on the SiO_2 core, controlled calcination experiments were performed. Pure CTS, pure SiO_2, and a series of CTS/SiO_2 core-shell supports with different mass ratios (1:5, 1:50, 1:100, 1:200) were calcined at 1000 ℃ for 6 h under a nitrogen atmosphere. The significant change of pure CTS (Figure S1) confirms its complete thermal decomposition at this temperature. In contrast, pure SiO_2 exhibits minimal mass change (Figure S2), highlighting its excellent thermal stability. For the core-shell supports (Figure S3), the observed mass loss systematically increases with the nominal CTS content, providing direct gravimetric evidence for the successful coating and controlled loading of the organic shell. The visual transformation—from the original samples to black carbonized residues after calcination for CTS-containing materials, while pure SiO_2 remains a white powder—further corroborates the uniform coverage of the silica core by the CTS layer.

Figure S1. Comparison of pure CTS samples before (left) and after (right) calcination at 1000 ℃.

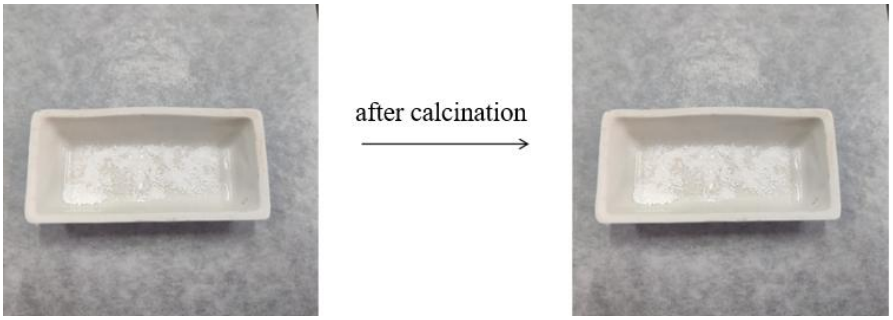

Figure S2. Comparison of pure SiO_2 samples before (left) and after (right) calcination at 1000 ℃

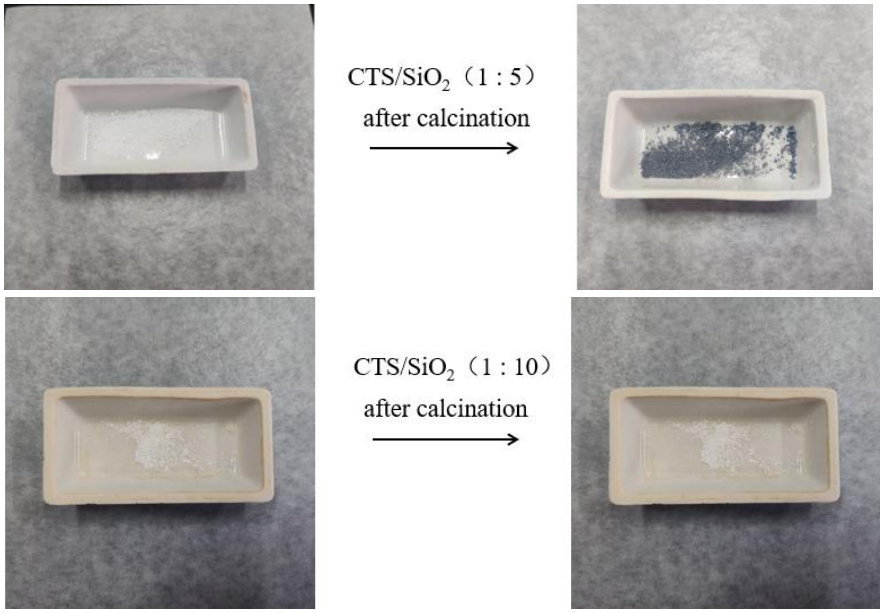

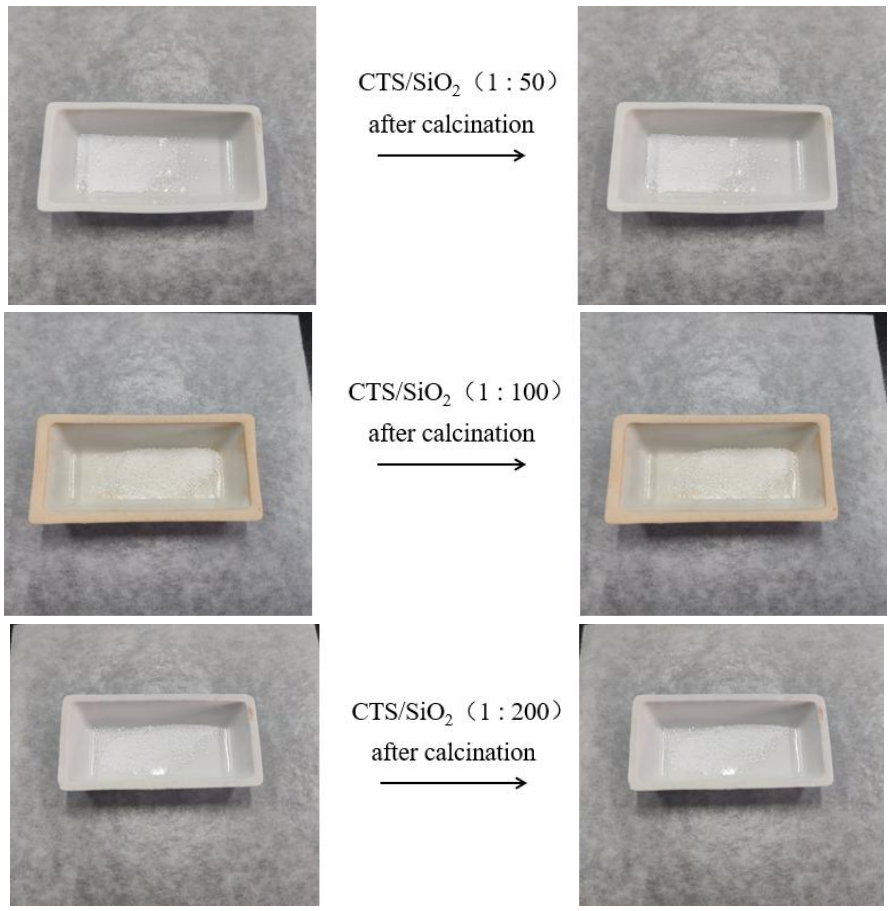

Figure S3. Comparison of different CTS/SiO_2 core-shell supports (ratios: 1:5, 1:50, 1:100, 1:200) before (left) and after (right) calcination at 1000 ℃

2. Particle Size Distribution Statistics and Numerical Data

Transmission Electron Microscopy (TEM) and subsequent elemental mapping (Pd) were employed to assess the dispersion of the palladium species. Figure S4 presents the particle size distribution histogram of Pd elements within the optimized 1% P-Pd@(CTS/SiO_2 1:100) catalyst, obtained by analyzing 100 randomly selected regions from the Pd map (see main text Figure 3e). The histogram, fitted with a Gaussian curve, shows a mean Pd particle size (or Pd-containing domain spacing) of approximately 11.05 nm with a standard deviation of ±3.98 nm. This distance is significantly larger than the molecular dimensions of a single Pd-porphyrin complex (~1.5 nm), providing strong statistical evidence for the molecular-level, non-aggregated dispersion of the active Pd sites within the CTS shell. The raw numerical data corresponding to this analysis are tabulated in Table S1.

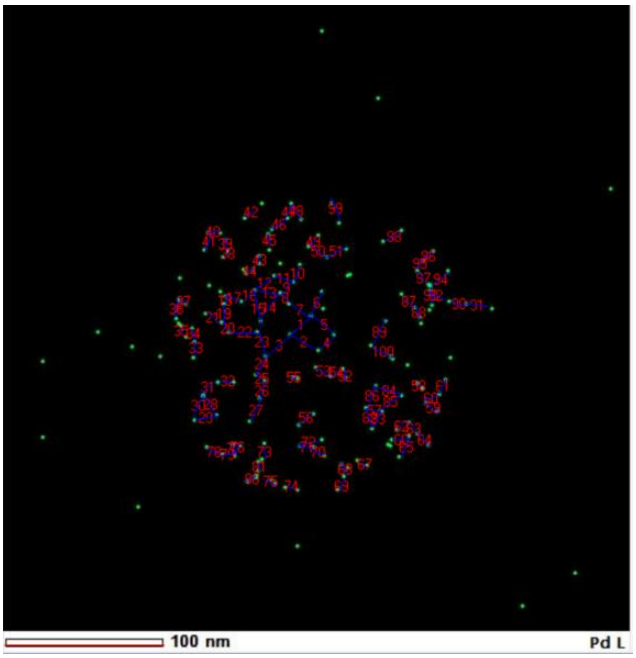

Figure S4. Particle size distribution histogram of Pd elements in 1% P-Pd@(CTS/SiO_2 1:100), derived from statistical analysis of the TEM-EDS map. The red line represents the Gaussian fit.

Table S1. Statistical data of particle size (d_{Pd}) distribution for 100 random Pd-containing domains from TEM-EDS analysis of 1% P-Pd@(CTS/SiO_2 1:100)

No.	d_{Pd}(nm)	No.	d_{Pd}(nm)	No.	d_{Pd}(nm)	No.	d_{Pd}(nm)
1.00	18.38	26.00	11.11	51.00	15.72	76.00	7.86
2.00	19.51	27.00	16.39	52.00	7.63	77.00	8.93
3.00	21.06	28.00	14.68	53.00	9.22	78.00	8.22
4.00	12.43	29.00	14.68	54.00	8.53	79.00	8.53
5.00	18.96	30.00	14.34	55.00	3.89	80.00	7.52
6.00	17.75	31.00	12.43	56.00	11.92	81.00	5.34
7.00	14.82	32.00	8.53	57.00	10.04	82.00	12.79
8.00	8.11	33.00	9.19	58.00	3.82	83.00	10.24
9.00	11.35	34.00	7.04	59.00	12.07	84.00	16.67
10.00	11.11	35.00	4.45	60.00	10.38	85.00	15.27
11.00	12.07	36.00	11.55	61.00	9.92	86.00	13.52
12.00	13.35	37.00	5.81	62.00	7.56	87.00	9.71

13.00	14.82	38.00	4.89	63.00	10.27	88.00	8.70
14.00	19.70	39.00	8.43	64.00	11.35	89.00	18.44
15.00	22.60	40.00	8.43	65.00	13.33	90.00	9.44
16.00	9.71	41.00	13.04	66.00	11.45	91.00	13.82
17.00	10.24	42.00	8.11	67.00	6.48	92.00	11.95
18.00	4.64	43.00	5.40	68.00	9.22	93.00	10.71
19.00	12.97	44.00	4.83	69.00	8.22	94.00	14.20
20.00	7.56	45.00	8.53	70.00	7.04	95.00	8.26
21.00	10.79	46.00	12.31	71.00	10.93	96.00	6.83
22.00	16.03	47.00	9.22	72.00	13.07	97.00	10.27
23.00	15.73	48.00	11.65	73.00	7.67	98.00	10.24
24.00	13.65	49.00	7.56	74.00	6.15	99.00	16.44
25.00	9.71	50.00	11.92	75.00	8.90	100.00	14.34

3. Mapping analysis

Energy-Dispersive X-ray Spectroscopy (EDS) mapping on a single catalyst particle provides visual confirmation of the core-shell architecture and the distribution of key elements. Figures S5 and S6 show the combined elemental maps and corresponding quantitative atomic ratio analysis for a representative 1% P-Pd@(CTS/SiO_2 1:100) particle. The Si signal (yellow) is concentrated in the core, defining the spherical support. The N signal (red), originating predominantly from the CTS shell and minimally from the porphyrin ligand, forms a uniform halo around the Si core, confirming the conformal coating. The Pd signal (blue) is dispersed homogeneously across the same region as the N shell, verifying the successful immobilization of Pd-porphyrin within the CTS layer. The quantified atomic ratios (N:Si:Pd ≈ 5.57:93.87:0.56) are consistent with a low, well-dispersed Pd loading within the N-rich organic matrix.

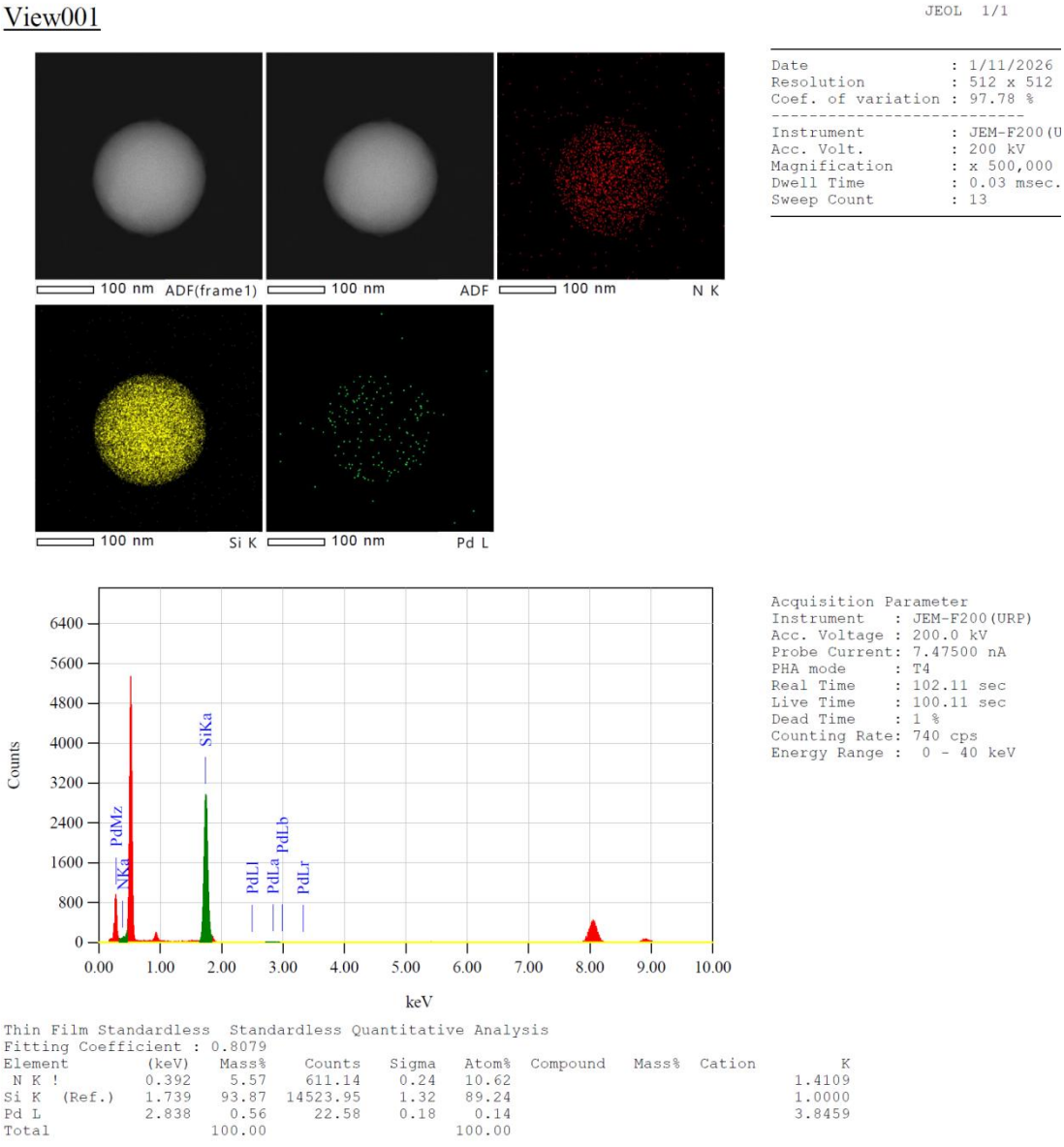

Thin Film Standardless Standardless Quantitative Analysis
Fitting Coefficient : 0.8079

Element	(keV)	Mass%	Counts	Sigma	Atom%	Compound	Mass%	Cation	K
N K !	0.392	5.57	611.14	0.24	10.62				1.4109
Si K (Ref.)	1.739	93.87	14523.95	1.32	89.24				1.0000
Pd L	2.838	0.56	22.58	0.18	0.14				3.8459
Total		100.00			100.00				

Figure S5. (top) Overlay of elemental maps (Si, N, Pd) for a single composite photocatalyst particle. (bottom) Corresponding quantitative atomic ratio analysis table for the mapped area.

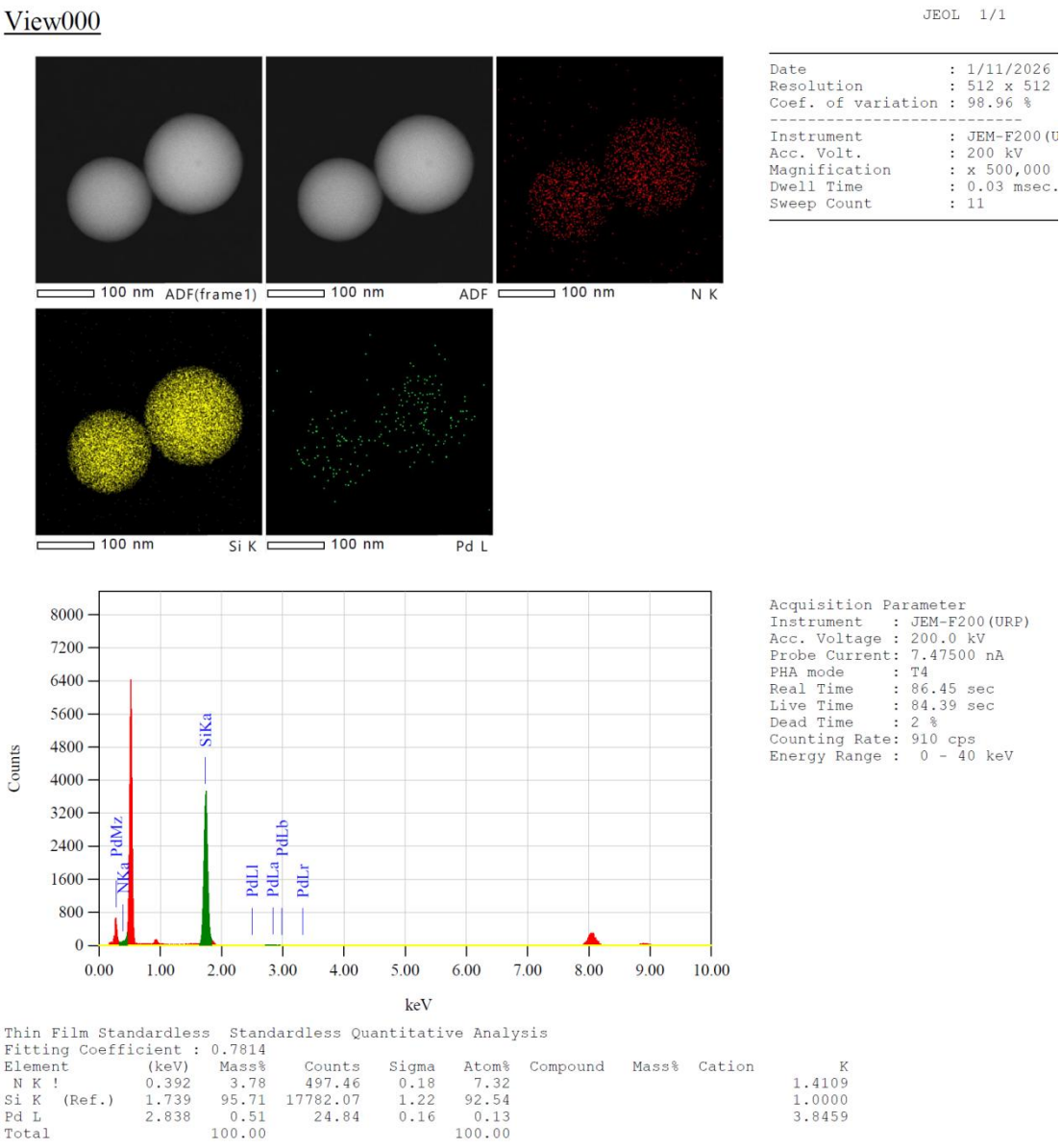

Figure S6. Individual elemental maps for (top) Si, N, and Pd from the same particle shown in Figure S5, along with (bottom) the quantitative atomic ratio analysis.

4. Effect of Active Component (P-Pd) Loading

To investigate the influence of catalyst loading on activity and to corroborate the monolayer immobilization concept, photocatalytic degradation of RhB was performed using P-Pd@(CTS/SiO_2 1:50) with varying nominal P-Pd loadings (1–4% w/w). As shown in Figure S7, the photocatalytic degradation profiles are nearly identical across this loading range. This insensitivity to catalyst loading strongly suggests that the active sites are predominantly located in a surface-accessible monolayer within the CTS shell. Once this monolayer is saturated (achieved even at 1% loading), additional P-Pd does not contribute significantly to activity, likely due to pore blockage or the formation of inactive aggregates, further supporting the effectiveness of the core-shell design in achieving optimal dispersion.

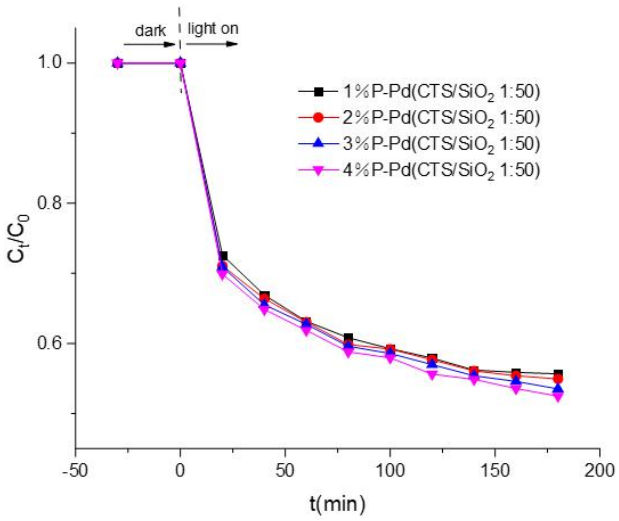

Figure 7 Photocatalytic degradation profiles of RhB over P-Pd@(CTS/SiO_2 1:50) with varying P-Pd loading ratios (1–4% w/w).

5. photocatalytic kinetic

The photocatalytic degradation process of Rhodamine B (RhB) was monitored by UV-Vis spectroscopy for catalysts with varying CTS/SiO_2 ratios (i.e., different shell thicknesses). Figure S8 shows the time-dependent spectral evolution. A gradual decrease in the characteristic RhB absorption peak at 554 nm is observed for all catalysts, indicating degradation. More importantly, distinct blue shifts of the absorption maximum are evident, the extent of which varies with the CTS/SiO_2 ratio. This spectral shift is a hallmark of the progressive N-dealkylation of RhB. The data in Figure S8 directly support the discussion in the main text regarding the tunable selectivity imparted by shell thickness: thinner shells favor controlled mono-dealkylation (smaller shift), while thicker shells promote deeper, multiple dealkylation pathways (larger shift).

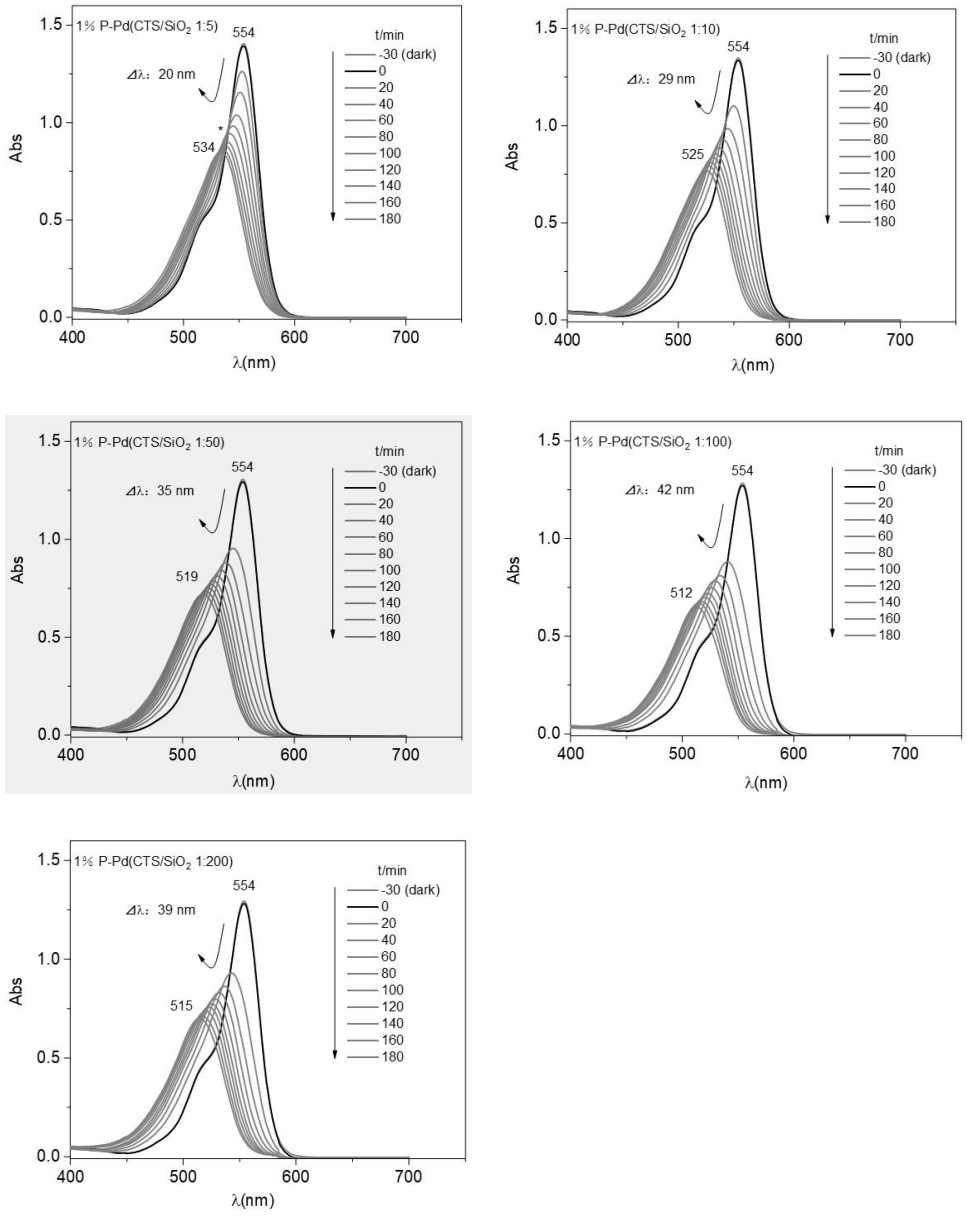

Figure S8. UV-Vis spectral evolution during the photocatalytic degradation of rhodamine B catalyzed by composite catalysts with different CTS/SiO_2 mass ratios: (a) 1:5, (b) 1:10, (c) 1:50, (d) 1:100, (e) 1:200.

6. Control Experiments: Adsorption and Photolysis

Control experiments were conducted to decouple photocatalytic activity from dark adsorption and direct photolysis. Figure S9 presents the dark adsorption profiles of RhB onto different CTS/SiO_2 supports (without P-Pd). All supports show negligible adsorption over 30 minutes, confirming that the observed RhB removal in photocatalytic tests is not due to physical adsorption. Figure S10 shows the RhB concentration changes under light illumination but in the absence of any catalyst ("Blank") or with pure supports. The minimal degradation observed in these control experiments confirms that the significant activity presented in the main text is exclusively attributable to the photoactive P-Pd species immobilized within the core-shell structure.

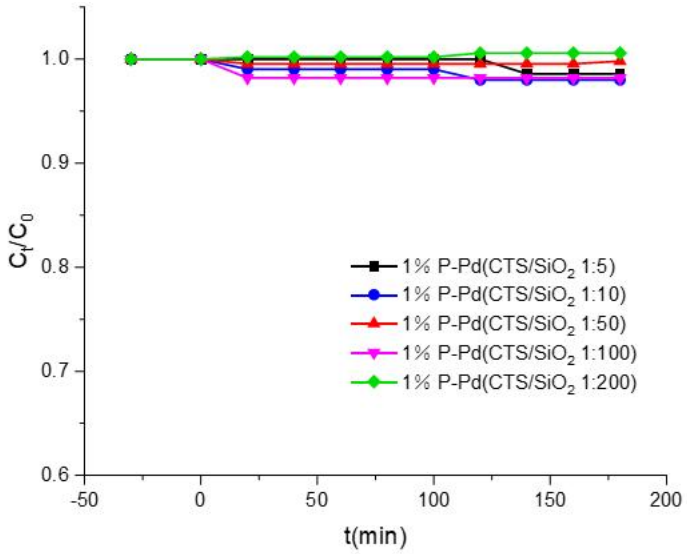

Figure S9. Dark adsorption profiles of rhodamine B on different ratios of CTS/SiO_2 composite supports (without P-Pd)

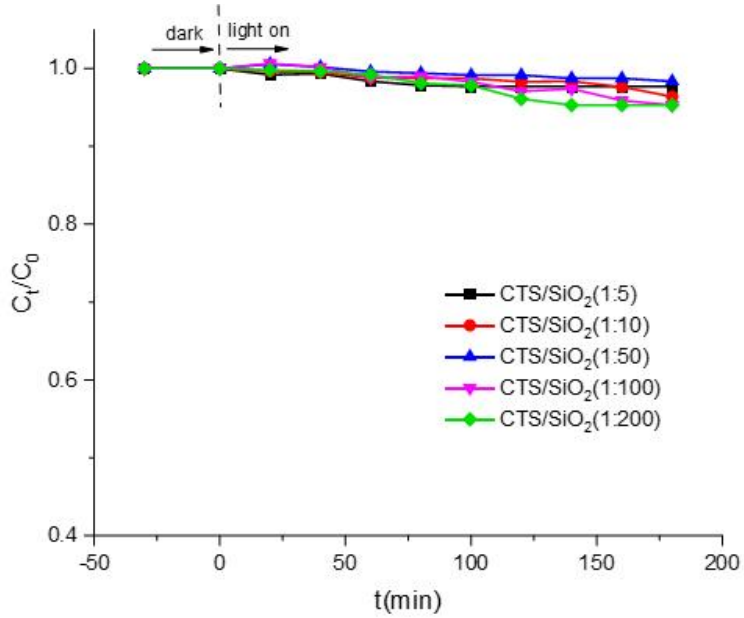

Figure S10. Photodegradation profiles of rhodamine B under light illumination for control systems: Blank (no catalyst) and pure CTS/SiO_2 supports with different ratios.